Experimental and numerical investigation of liquid jets evaporating in a dilute gas–liquid–solid pipe flow

W. Arnold, S. Wirtz & V. Scherer
Department of Energy Plant Technology (LEAT),
Ruhr-University Bochum, Germany

Abstract

The application of selective noncatalytic reduction (SNCR) in modern cement plants is complex, since the evaporating additive is injected into a highly particle-laden hot gas stream and therefore the conventional two phase evaporation approach may not be adequate to describe the system. After a collision with a particle, the droplet is either fully evaporated or a wetted particle is formed, depending on the difference of particle size and particle heat capacity with respect to gas and liquid phases. This can result in a deviation of the jet penetration depth from the conventional two phase (gas/liquid) theory. Experiments were conducted to examine the behavior of liquid jets evaporating in a gas–liquid–solid pipe flow. The test facility consists of a vertical pipe in which a continuous flow of quartz sand particles and hot air in thermal equilibrium is established. Water is injected into this stream by a pressure nozzle in co-flow with the gas solid stream. The evaporation is investigated with thermocouples. Effects of solids loading and system temperature on the jet evaporation behavior will be presented. In order to consider the measured effects in CFD simulations, an existing stochastic particle collision model has been extended to account for droplet–particle interaction in three-phase flows. This model predicts the probability of droplet–particle collisions and in case of collision, droplet movement and evaporation behavior change. Comparisons with the experimental data show that this model can predict reasonable results for the temperature distribution for various operational conditions.
Keywords: evaporation, particle–droplet-interaction, gas–liquid–solid flows, cfd-simulation.

1   Introduction

High process temperatures and the use of nitrogen containing fuels have the consequence that, without secondary reduction measures, process-related NO_x contents in the exhaust gas of rotary kilns in the cement industry would considerably exceed the current specifications of the German Emissions Directive of 200mg/m^3. Even with staged combustion and the selective noncatalytic reduction (SNCR) technique the current emission limit for NO_x poses a challenge for the industry and makes the optimization of the SNCR technique in cement plants essential [1].

For the injection of the liquid reduction agent the calciner tends to be the optimal position, since the temperature level resulting from the calcination of the limestone lies within the optimal temperature window of the reduction reaction. However, the injection of a liquid into such a highly particle-laden hot gas stream makes a description of this complex system difficult, since liquid–solid interactions must be considered. Especially for a mixing sensitive technique like SNCR, the understanding of the evaporation behavior and the subsequent mixing is the key element for high NO_x reduction levels. Only if the dominant transport mechanism is understood, proper nozzle parameters (pressure, cone angle) and an injection position resulting in an even dispersion of the reduction agent can be set.

2   Experimental setup

The experimental setup is designed to investigate the particle–droplet-interaction in a heated gas–liquid–solid system. As illustrated in figure 1, the key element of the experiment is the measuring section, which consists of a vertical pipe with a height of around 2m and an inner diameter of 163mm, in which a continuous flow of particles and hot air in thermal equilibrium is established. The air is supplied by a compressor and controlled with a bypass to a maximum volumetric flow of 200m^3/h. An electrical air heater is used to heat the air to a maximum temperature of 200°C. The quartz sand particles with a mean diameter of 110µm are continuously conveyed by a screw-driven powder feeder with a maximum flow rate of 50kg/h. The distance from the injection point to the measuring section is sufficiently large to assure that gas and particles are well-mixed. At a height of 0.658m water is injected by a pressure nozzle in co-flow with the gas–solid stream. The single-fluid nozzle used is a hollow cone nozzle manufactured by Bete GmbH in Bochum with a cone angle of 63° and a Sauter mean droplet size of approximately 40µm at an injection pressure of 8 bar. A thermocouple located upstream of the injection point was used for temperature control of the entering particle laden stream. The evaporation behavior is investigated with thermocouples (1.5mm Type K) in a measurement area covering a distance of approximately 1m downstream of the injection point. The radial positon of the thermocouples can be varied in order to obtain horizontal profiles of the temperature field. Alternatively to the temperature measurement the modularly constructed measuring section can be equipped with a glass

module, allowing a visual observation of the particle and droplet distribution. After the measuring section, particles and air are separated in a cyclone and the particles are returned to the particle bunker. The separated air is than filtered and released to the environment.
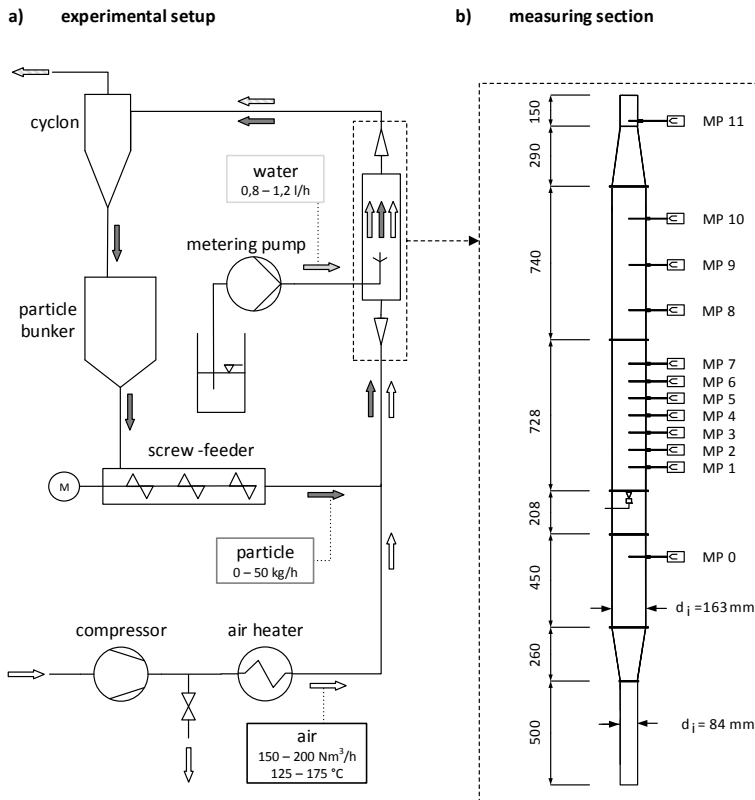

Figure 1: Scheme of a) the experimental setup and b) the measuring section.

3 Experimental data and discussion

The influence of the particulate phase on the evaporation behavior was investigated by comparing measured axial temperature profiles of the following four cases.

Table 1: Overview of the operating conditions.

	V1	V2	V3	V4
Temperature (MP 0)	150°C	150°C	150°C	150°C
Volume flow air	150 Nm³/h	150 Nm³/h	150 Nm³/h	150 Nm³/h
Mass flow particle	0 kg/h	50 kg/h	0 kg/h	50 kg/h
Volume flow water	0 l/h	0 l/h	1.2 l/h	1.2 l/h

The experimental results are illustrated in figure 2. The settings V1 and V2 show almost the same temperature distribution with an overall heat loss in the facility of around 2°C. By injecting water through the nozzle (V3 and V4), the temperature drops due to the evaporation heat sink. Especially for the measuring points close to the injection, a constant temperature of around 40°C is measured. This indicates that these thermocouples are wetted, which was confirmed by visual inspection through a glass module. In figure 2 the temperatures for the settings V3 and V4 show a similar trend, but the temperatures in V4 are slightly higher in the spray core (dense droplet vapor zone) and continuously reduce further downstream. The higher temperatures can be explained by the heat capacity of warm particles sticking to the wetted thermocouple. Note that the lower temperature cannot be explained solely with the heat capacity and indicates a difference in the evaporation.
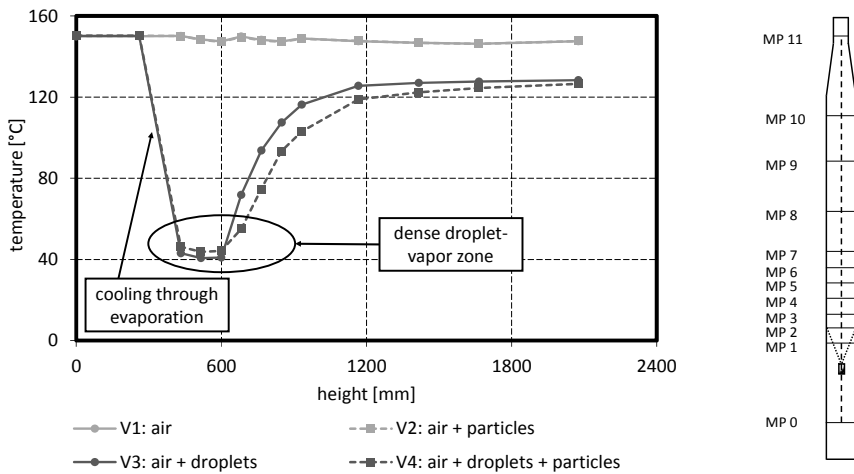

Figure 2: Measured temperature distribution along the centreline.

For the interpretation of the observed results a one dimensional evaluation is not sufficient, since the spray pattern of a hollow cone nozzle is at least a two-dimensional problem and therefore the radial temperature distribution has to be considered. In figure 3 the measured data of cases V3 and V4 are illustrated as contour plots. In addition the measuring points and the required mesh for interpolation are presented. It can be seen that for the three phase flow the temperatures tends to be lower in the near field of the injection. This indicates that the combination of particle–droplet interactions and the additional heat transfer capability carried by the particles promote evaporation. Similar observations are documented by Zhu et al. [2]. However, the geometric characteristics of the hollow cone nozzle lead to a narrower, but axially more extended evaporation zone.
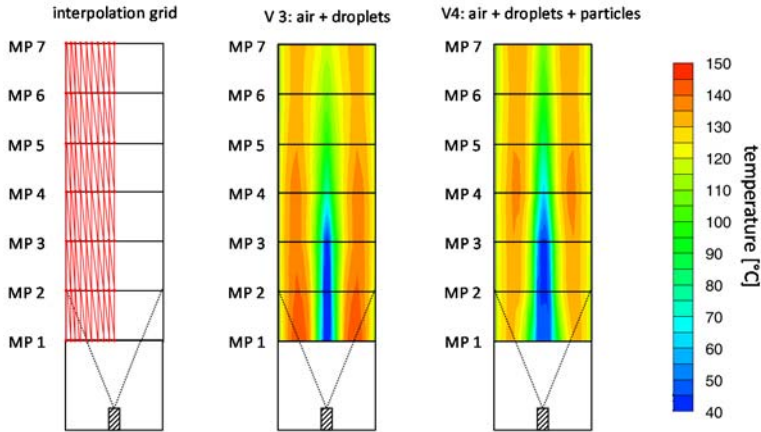
Figure 3:   Vertical distribution of the measured temperature.

3.1 Variation of inflow temperature

The results of an inflow temperature variation (125–175°C) are illustrated in figure 4. Besides the temperature, all other conditions have been kept according to table 1. It can be seen that the length of the dense droplet–vapor zone varies with the gas phase temperature, which is an expected result since the temperature is

the dominant parameter for the evaporation time of a water droplet. Furthermore, the temperature measured in this zone is nearly independent of the inlet
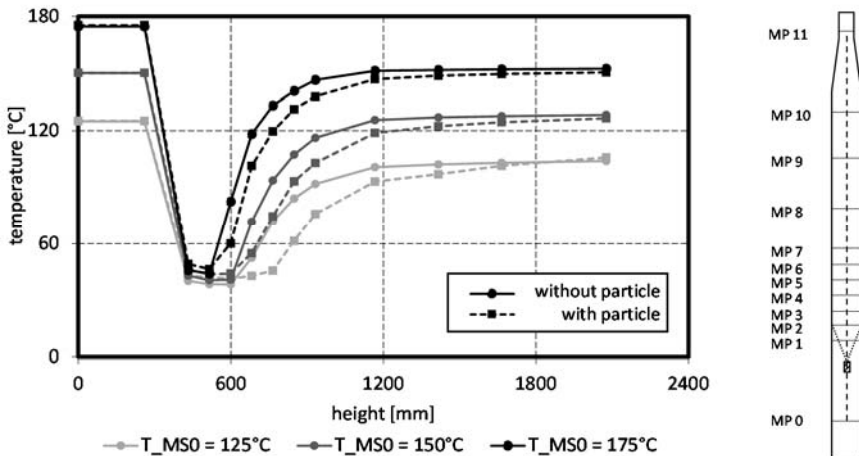

Figure 4:   Variation of gas phase temperature.

temperature supporting the conclusion of wetted thermocouples. Generally, the comparison between two and three phase flows show at first glance a similar structure, however depending on the gas temperature the extent of the cooler regions varies. Especially for the low 125°C inlet temperature the interaction with the particles results in an obviously longer dense droplet–vapor zone along the centreline of the measuring section. This variation indicates that the difference between the two and three phase flow becomes less distinctive with higher system temperatures, since the evaporation occurs faster and therefore less time for particle–droplet interactions remains.

3.2 Variation of particle and droplet concentration

In additional measurement series the influence of particle and droplet concentration on the temperature distribution was investigated. The results are summarized in figure 5. For a simplified depiction the temperature ratio according to equation 1 has been chosen.

$$ratio = \frac{Temperature\ without\ particles}{Temperature\ with\ particles} \qquad (1)$$

A variation of the particle mass flow a) shows that for higher particle loadings the ratio outside of the dense droplet-vapor zone tends to have a smaller value, which means that the deviation from the conventional two phase evaporation becomes larger. A similar observation can be made by varying the water mass flow b), since the larger water mass flow tends to result in smaller values independent of the gas temperature. These variations show that both, the particle and the droplet loading have a significant influence on the temperature difference. With respect to particle–droplet interactions, this observation is in accordance with general collision models, since the collision probability is mainly dependent on the number density of particles or droplets.
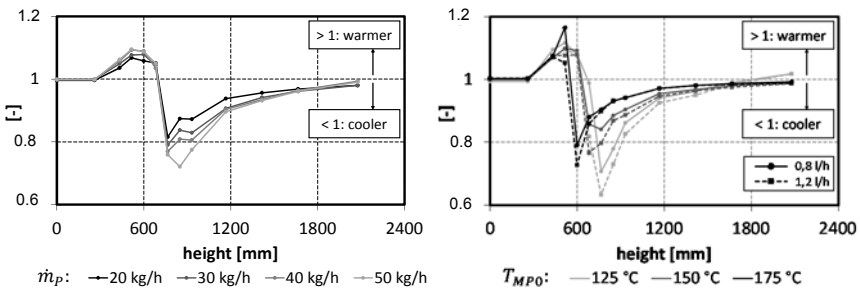

Figure 5:   Variation of a) water mass flow and b) particle mass flow.

4   Simulation boundaries and numerical modelling

Steady-state simulations of the experimental setup were performed using the commercial CFD software package ANSYS FLUENT (Version 14.5). The continuous phase is modelled as a mixture of nitrogen, oxygen and water vapor.

For the turbulent flow the k-ω SST turbulence model is chosen, thermal radiation is neglected due to the low overall temperature level. The measuring section is discretised using approximately 700,000 hexahedral control volumes with a higher spatial resolution in vicinity of the injection region.

The solid and liquid phase are expressed with the Discrete Phase Model (DPM), in which the particle and droplet trajectories are predicted by integrating the force balance on the particle in a Lagrangian frame. For both phases the random effects of gas phase turbulence on the particle dispersion is accounted for by the Discrete Random Walk (DRW) model. The solid phase is simulated as inert particles with a given diameter distribution. For the injection boundary the Linearized Instability Sheet Atomization (LISA) model, which computes the droplet velocity and diameter distribution after film formation and sheet breakup, has been chosen [3]. The resulting droplet distribution was compared with the droplet distribution of the nozzle used (measured with a PDA-system) and showed reasonable agreement. Droplet evaporation and boiling are simulated with the models available in the software package. A user defined function (udf) was developed which considers the particle–droplet-interaction and a virtual thermocouple temperature. Both approaches are described in the following sections.

4.1 Modelling particle–droplet interaction

In order to describe the interaction between the solid and the liquid phase a stochastic collision model based on the Euler/Lagrange approach was implemented. This model extends the inter-particle collision model of Sommerfeld [4, 5] such that droplet-particle collisions are included. Analogously to the Sommerfeld model a fictitious potential collision partner, in this case a solid particle, is generated in every time step of the simulated droplet trajectory and a collision probability according to kinetic theory is calculated. The advantage of this model is that information's on the actual locations of all surrounding particles are not required. Thus, it is also applicable if a sequential tracking of the particles is adopted. The collision probability P_{coll} of the actual tracked droplet (P1) and a fictive solid particle (P2) is a function of the collision frequency and the Lagrangian time step and is defined as follows:

$$P_{coll} = f_c \Delta t = \frac{\pi}{4} \cdot (d_{P1} + d_{P2})^2 \cdot |\overrightarrow{v_{P1}} - \overrightarrow{v_{P2}}| \cdot n_P \, \Delta t \qquad (2)$$

The fictive solid particle is a representative of all solid particles in the current control volume. Therefore the required information, as the diameter d_{P2} and the velocity $\overrightarrow{v_{P2}}$, must be stored as cell information after every particle iteration step. For every value two parameters are stored analogous to equation 3, namely the mean value and the standard deviation and the actual value is calculated using a normally distributed random number χ.

$$d_{P2} = \overline{d_P}\big|_{(n)} + \sigma_{d_p} \cdot \chi \qquad (3)$$

The particle number density n_P is defined as the number of solid particles in every calculation cell per cell volume V_{cell}. Since individual particles are packed in trajectories, the total number is calculated through a summation of the trajectory particle number rate $\dot{n}_P$ and the particle residence time in that cell Δt_{cell}.

$$n_P = \frac{1}{V_{cell}} \sum_{i=1}^{n_{Traj.}} \dot{n}_P \, \Delta t_{cell} \tag{4}$$

If a collision occurs, various options are possible, as illustrated in figure 6. The outcome depends on the difference of droplet to particle size and the particle surface structure. If, for example, a small particle and a large droplet collide, the particle will be absorbed by the large droplet, but if particle and droplet have similar diameters, the droplet will form a film on the particle surface. For the current target system option b and c are the most likely, since the particle to droplet diameter ratio is almost two. To determine the post-collision velocities, the momentum transferred between the droplet and the particle has to be determined. For simplification, the collision occurs non-sliding. Since the deterministic collision is calculated according to the Sommerfeld model, a detailed description of the collision computation is not presented in this study.
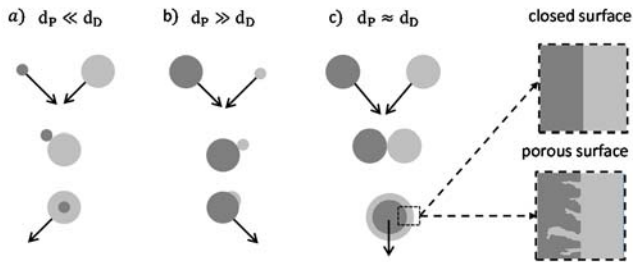

Figure 6:   Schematic illustration of possible particle droplet collisions.

Besides the particle movement, the evaporation conditions may change. For a non-porous particle the liquid forms a film around the particle and the evaporation takes place at the particle's surface. For porous particles the liquid may be sucked into the particle's pores, depending mainly on the surface tension ratio of all involved phases. In this study the quartz sand particles have a closed surface and the evaporation takes place at the particle's surface. This is considered in the simulation through an adjustment of the evaporation model, in which basically the surface area for the evaporation is changed according to the particle diameter and the resulting film thickness.

An example for the interaction between particles and droplets is presented in figure 7c). For both pure two phase flows (a and b) trajectories are simulated as expected. If particle–droplet collisions are additionally considered, the movement of the droplets deviates from the pure two phase flow (middle). Several droplets collide with particles, illustrated by a colour change, and change their path. This results in higher droplet concentrations along the centreline of the flow field.

a) air + particles   b) air + droplets   c) air + droplets + particles
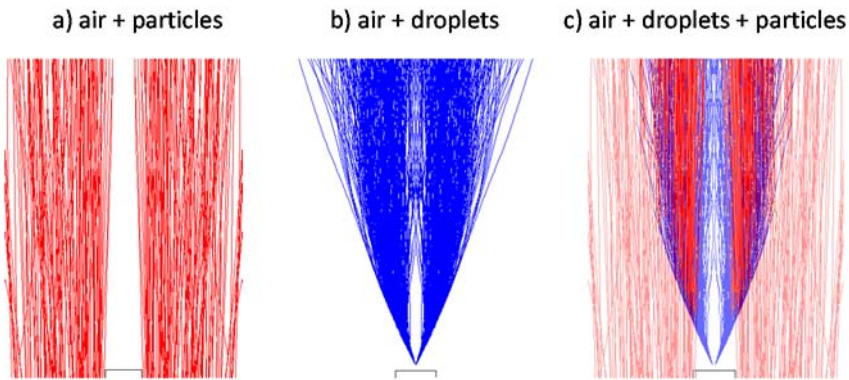

Figure 7: Influence of the particle-droplet interaction on the droplet movement.

5   Comparison between experimental and numerical results

Figure 8 compares the simulated and measured temperature distribution for the single phase and the two phase flow along the centreline of the measuring section. For the settings V1 (air) and V2 (air + particle) an almost even distribution with a very good agreement between experimental and numerical results can be depicted, which indicates that heat losses are adequately simulated. In contrast, the comparison of the simulated gas phase temperature (GT) and the experimental data for the setting V3 (air + droplet) shows, especially in the dense spray region, only a poor agreement, since the thermocouples are most likely wetted. Thus the thermocouples reflect the temperature of the evaporating liquid. To correct these data, a virtual thermocouple temperature was defined in the simulations, which accounts for the droplet concentration c_D in the gas phase according to equation 5.

$$T_{VT} = T_{gas} * (1 - a) + \bar{T}_{Droplet} * a \tag{5}$$

with:

$$a = \begin{cases} c_D * 50 & , c_D \leq 0{,}02 \ kg/m^3 \\ 1 & , c_D > 0{,}02 \ kg/m^3 \end{cases} \tag{6}$$

With these "virtual" thermocouple temperatures (VT), reflecting the partial wetting of thermocouples, the results converge to the measured temperature distribution. A similar pattern can be seen in the temperature distribution in a vertical plane through the measuring section, see figure 9. The good agreement with the measurements confirms that the approach is appropriate for the simulation if only evaporation is considered.
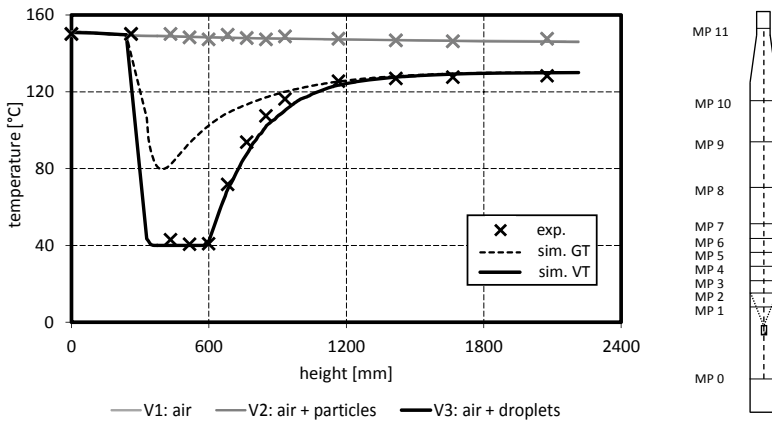
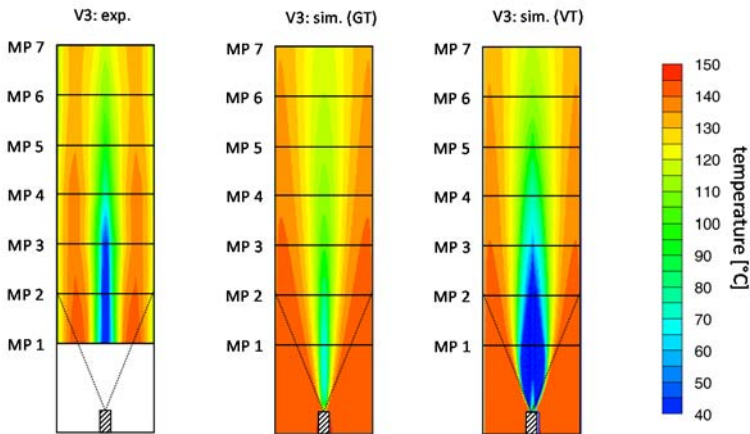Figure 8: Measured and simulated temperature distribution along the centreline.

Figure 9: Vertical distribution of the measured and simulated temperature.

Figure 10 compares the simulated and measured temperature distribution in the three phase flow (V4) compared with sole evaporation in hot air (V3). It becomes visible, that for the standard case without particle–droplets interaction, the simulated temperatures are much higher than in the reference case with evaporation alone. The reason for this effect is the additional heat capacity of the particles. Since the spray pattern does not change, a generally higher temperature distribution exists. By considering the particle–droplet interaction the temperature distribution changes to lower values showing a better agreement with the experimental data. This is also evident in the vertical distribution of the measured and simulated temperatures, which are pictured in figure 11.
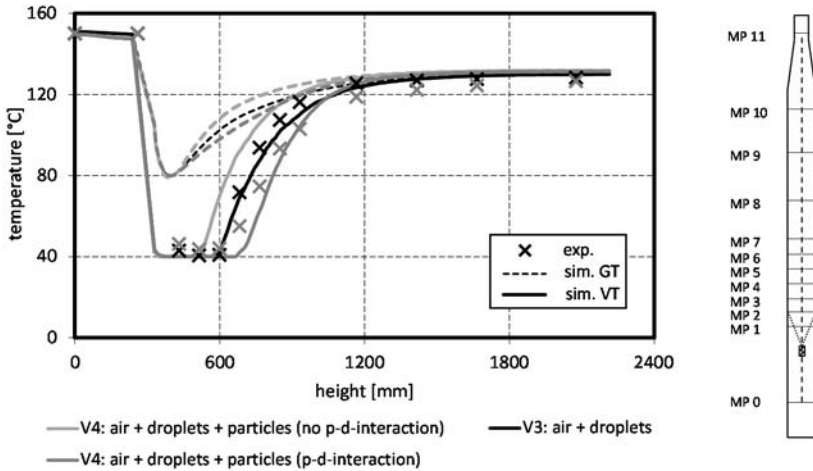
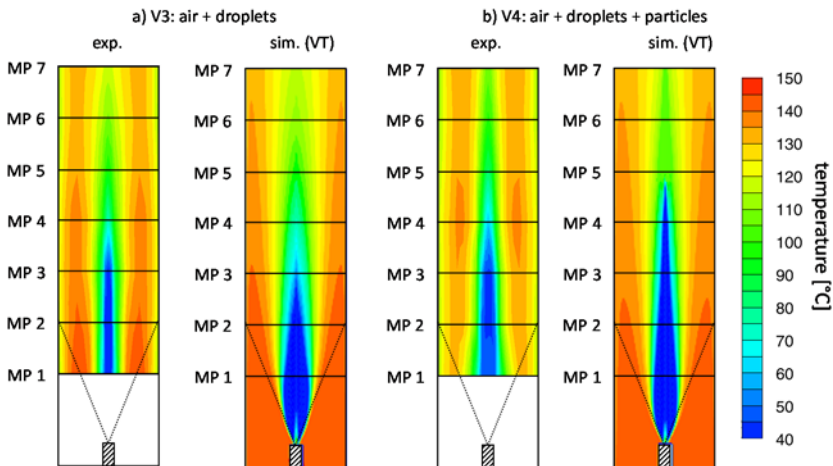Figure 10: Measured and simulated temperature distribution along the centreline.

Figure 11: Vertical distribution of the measured and simulated temperature.

6   Summary and conclusions

In this study the evaporation of a liquid jet injected into a dilute gas–liquid–solid pipe flow was investigated experimentally and numerically. For this purpose a vertical measuring section was constructed, which allows controlled variations of the gas phase temperature as well as the particle and droplet concentration. The evaluation of the evaporation behavior with and without particles revealed a

change in the measured temperature distribution. The particle droplet interactions seem to promote the evaporation, which in the case of the hollow cone nozzle used, results in a narrower and longer evaporation zone, due to the geometric characteristics of the hollow cone nozzle used. A sensitivity analysis of the particle and droplet concentration showed that this phenomenon strongly depends on the particle and droplet concentration.

In order to consider the particle–droplet-interaction in CFD simulations, a stochastic droplet–particle interaction model for three-phase flows has been implemented in the context of the Euler/Lagrange approach. This model predicts the probability of droplet–particle collisions and, in case of a collision, changes the droplet movement and the evaporation characteristics. A comparison with the experimental data shows, that this model can predict reasonable results of the temperature distribution for various operational conditions.

Further numerical studies will investigate the effect of the particle–droplet interaction introduced on evaporating additives, as used in the SNCR technique, in a full scale calciner.

Acknowledgement

References

[1] Verein Deutscher Zementwerke (VDZ), Environmental Data of the German Cement Industry 2013, 2014.
[2] Zhu, C., Wang, X. and Fan, L.S., Effect of solids concentration on evaporative liquid jets in gas–solid flows. Powder Technology, 111, pp. 79–82, 2000.
[3] Schmidt, D.P., Nouar, P.K., Senecal, P.K., Rutland, C.J., Martin, J.K. and Reitz, R.D., Pressure-Swirl Atomization in the Near Field, SAE Paper 01–0496, 1999.
[4] Sommerfeld, M., Validation of a stochastic Lagrangian modelling approach for inter-particle collisions in homogeneous isotropic turbulence, International Journal of Multiphase Flow, 27, pp. 1829–1858, 2001.
[5] Sommerfeld, M., Modellierung und numerische Berechnung von partikelbeladenen turbulenten Strömungen mit Hilfe des Euler-Lagrange-Verfahrens, Shaker Verlag: Aachen, 1996.